Reaction Chemistry & Engineering

ROYAL SOCIETY OF CHEMISTRY

PAPER

View Article Online
View Journal | View Issue

Cite this: *React. Chem. Eng.*, 2020, 5, 1759

Bifunctional carbon Ni/NiO nanofiber catalyst based on 5-sulfosalicylic acid for conversion of C5/C6 carbohydrates into ethyl levulinate†

Haixin Guo, *[a] Yuya Abe, [a] Xinhua Qi [b] and Richard Lee Smith Jr *[ac]

Received 19th April 2020,
Accepted 30th July 2020

DOI: 10.1039/d0re00153h

rsc.li/reaction-engineering

A method was developed for preparing bifunctional carbon Ni/NiO nanofiber catalysts that promote efficient one-pot conversion of C5/C6 carbohydrates into levulinate esters in alcohol solvents. The bifunctional catalysts were prepared *via* solvothermal carbonization of 5-sulfosalicylic acid/$NiSO_4$ without the use of sulfuric acid or hydrogen gas and had fine particle sizes (d = 5 nm to 50 nm) and contained $-NH_2$, $-SO_3H$, –COOH and phenolic –OH functional groups. Under optimal conditions, the catalysts afforded 93% selectivity of ethyl levulinate in ethanol with the major intermediate being 2-(ethoxymethyl) furan, 4,5,5-triethoxypentan-2-one and major byproduct being 2,5,5-triethoxpentan-2-one. Cooperative activity of Lewis acidity, Brønsted acidity and functional group sites of the catalyst is demonstrated for multi-step reaction sequences of C5/C6 carbohydrates with one-pot conversions and alcohols (methanol, ethanol, 1-propanol, 1-butanol) that act as both solvent and hydrogen donor source in which the bifunctional catalyst was shown to be recyclable five times with no apparent change in conversion and *ca.* 5% change in selectivity.

1. Introduction

Conversion of lignocellulosic biomass into fuels and platform chemicals is a multi-step process that requires delignification and hydrolysis of cellulose and hemi-cellulose portions to produce C5 (pentose) and C6 (hexose) sugars[1] that are challenging to separate or convert into respective value-added chemicals. In previous studies, catalysts applicable to the conversion of carbohydrates into furfural,[2,3] 5-hydroxymethylfurfural (5-HMF),[4–6] 5-ethoxymethylfurfural (5-EMF),[4,7] levulinates,[8] γ-valerolactone (GVL),[9–11] and other important oxygen-containing platform molecules[12] have been reported. Much effort is required for separating and purifying mixed raw sugars into C5 and C6 carbohydrate fractions[13] and these carbohydrates have differences in their downstream products. Bifunctional catalysts with different active sites (acidity sites and metal sites on same catalyst) can be used advantageously to avoid intermediate separation and purification steps for targeted products.

Among the products that can be obtained from C5/C6 carbohydrates, ethyl levulinate (EL) is particularly promising, because it can be used as a solvent, plasticizer, fuel additive or further transformed into value-added chemicals such as GVL.[9,14] EL has a lower cloud point than biodiesel and it can greatly improve cold flow properties of biodiesel.[8] In a reaction scheme with a bifunctional catalyst, C6 carbohydrates can be converted into EL by acid catalyst *via* dehydration–ethanolysis with 5-HMF and levulinic acid (LA) as intermediates,[15] while C5 carbohydrates can be converted into EL by acid–metal catalyst *via* dehydration–reduction–ethanolysis–decomposition with furfural and furfuryl alcohol (FAL) as intermediates.[14,16] Many reports have been made on conversion of C5/C6 carbohydrates into EL with using acid ionic liquids[16] or with mineral acids.[2] However, conversion of C5/C6 carbohydrates with bifunctional catalysts in one-pot offers the hope of simplifying process chemistry and improving reaction efficiency.

The compound, 5-sulfosalicylic acid (5SA), has three different functional groups (–OH, $-CO_2H$ and $-SO_3H$) that can coordinate with metals in many ways to form definitive structures,[17–19] thus making it highly versatile for synthesizing metal organic-frameworks when combined with suitable linkers.[18] When 5SA is used with metals as substrate without a linker, it has the potential to form a kind of template for preparing bifunctional catalysts that allows

[a] *Graduate School of Environmental Studies, Tohoku University, Aramaki Aza Aoba 6-6-11, Aoba, Sendai 980-8579, Japan. E-mail: haixin-g@scf.che.tohoku.ac.jp, smith@scf.che.tohoku.ac.jp; Fax: +81 022 795 5864, Fax: +81 022 795 5863; Tel: +81 022 795 5864, +81 022 795 5863*

[b] *College of Environmental Science and Engineering, Nankai University, No. 38, Tongyan Road, Jinnan District, Tianjin 300350, China*

[c] *Research Center of Supercritical Fluid Technology, Tohoku University, Aramaki Aza Aoba 6-6-11, Aoba-ku, Sendai 980-8579, Japan*

† Electronic supplementary information (ESI) available: Details of the XPS, SEM, EDX, TG-DTA, GC-MS, FT-IR, ^{1}H NMR and carbon balance analyses are given in ESI. See DOI: 10.1039/d0re00153h

introduction of Brønsted acidity sites into their structure.[20] In this work, we show that bifunctional catalysts with Lewis acidity and Brønsted acidity sites can be readily synthesized with 5SA and demonstrate the conversion of C5/C6 carbohydrates into ethyl levulinate or related levulinate esters.

In this work, a method is developed for synthesizing carbon Ni/NiO nanofiber catalysts that have Lewis and Brønsted acidity sites. The catalyst has Ni/NiO sites that are functionalized with $-NH_2$, $-SO_3H$, –COOH and –OH groups. The resulting bifunctional carbon Ni/NiO nanofiber material is robust and reusable and has high catalytic activity in alcohol solvents for one-pot conversion of C5/C6 carbohydrates into EL or into LA-esters.

2. Experimental

2.1. Materials

Levulinic acid (LA, 99%), furfuryl alcohol (FAL, 98%), furfural (99%), D-fructose (98%), sucrose (99.5%), 2-(ethoxymethyl) furan (2-EMF), furfural diethyl acetal (FDA, 98%), methanol (99.95%), ethanol (99.5%), 1-propanol (99.5%), 1-pentanol (98.0%), 1-butanol (99.0%), *N*,*N*-dimethylacetamide (DMA, 97%), nickel(II) sulfate hexahydrate (99%), 5-sulfosalicylic acid dehydrate (5SA, 99%), and dodecane (>99%) were obtained from Wako Pure Chemical Industries, Ltd. (Osaka). Ethyl levulinate (EL, 99%) and microcrystalline cellulose (MCC, CAS number 9004-34-6, particle size 51 μm) were obtained from Sigma-Aldrich (Japan).

2.2. Catalyst preparation

The catalytic material was prepared in a single-step by solvothermal reaction of 5SA with nickel(II) sulfate hexahydrate in DMA. Typically, 1 mmol of 5SA, 1 mmol of metal salt, and 30 mL of DMA were added into a Teflon-lined stainless-steel autoclave (100 mL) and maintained at 120 °C for 10 h. The products were isolated by centrifugation and washed in ethanol several times, followed by oven-drying at 60 °C for 24 h. The resulting solids were ground to powder and heated at 500 °C for 2 h under a pure nitrogen gas atmosphere that was followed by cooling of the solid and repeated washings with distilled water. The calcined black solids were dried at 60 °C for 24 h.

2.3. Catalyst characterization

Total acidity of the as-prepared catalyst was analyzed with the Boehm method.[21] Surface topography of as-prepared catalysts was investigated with scanning electron microscopy (SEM, Hitachi S4800) at 5.0 kV and transmission electron microscope (TEM, Hitachi HD-2700, type-B) at 200 kV. The TEM samples were prepared by dropping dilute solutions transferred in ethanol onto a copper grid (ELS-C10, 100 μm) with excessive ethanol being immediately evaporated. X-ray diffraction (XRD) measurements were performed with a Rigaku diffraction system (MiniFlex) with Cu Kα radiation operated at 30 kV and 15 mA with scattering slit at 4.2°. Surface elemental valence analysis was performed using X-ray photoelectron spectroscopy (XPS, Axis-Ultra, Shimadzu) with a pass energy of 20 eV and 200 times acquisition. Thermal gravimetric and differential thermal analysis (TG-DTA) measurements were carried out between room temperature and 500 °C at a heating rate of 10 °C min^{-1} under an N_2 flow on Seiko TG/DTA 6200 (Japan) instrument. FT-IR spectra (FT-IR-230, JASCO) were recorded from 400 cm^{-1} to 4000 cm^{-1} and with a resolution of 4 cm^{-1} after materials were evenly mixed with KBr powder and compressed into pellets.

2.4. General experimental procedure

For a typical run, 0.1 g substrate (*ca.* 1 mmol furfuryl alcohol), 3 mL or 5 mL alcohol as solvent/reactant and 0.05 g of as-prepared catalyst were added into a Teflon-lined stainless-steel autoclave (15 mL). The reaction mixture was stirred at (140 to 160) °C and after a given reaction time, the autoclave was cooled in an ice bath, opened and its contents were diluted with ethanol and filtered before being analyzed with GC-MS/FID using dodecane as internal standard for product analysis (section 1, ESI†). Definitions of conversion, yield and selectivity are given as follows:

$$\text{Conversion (mol\%)} = \left(1 - \frac{\text{moles of remaining reactant}}{\text{initial moles of reactant}}\right) \times 100\% \quad (1)$$

$$\text{Yield (mol\%)} = \frac{\text{moles of product}}{\text{initial moles of reactant}} \times 100\% \quad (2)$$

$$\text{Selectivity (\%)} = \frac{\text{Yield}}{\text{Conversion}} \times 100\% \quad (3)$$

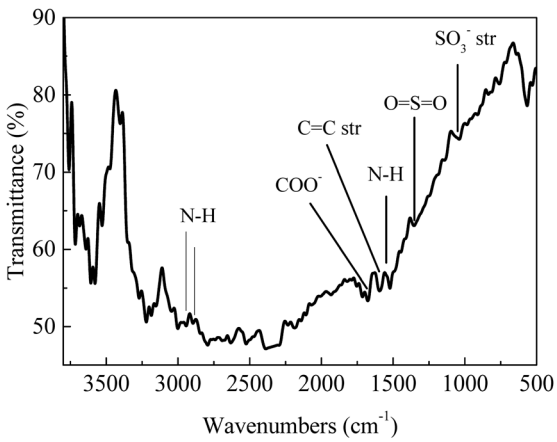

Fig. 1 FT-IR spectrum of as-prepared bifunctional carbon Ni/NiO nanofiber catalysts.

3. Results and discussion

3.1. Characterization of catalyst

FT-IR analysis (Fig. 1) of the solids showed bands around 3400 cm^{-1} that are characteristic of stretching vibrations of hydroxyl –OH groups.[22] Vibration bands at 1690 cm^{-1} and 1603 cm^{-1} are attributed to carboxyl group and C═O stretching vibrations, respectively, indicating that the solids were functionalized with $–COO^-$ and –OH groups.[22,23] Occurrence of bands at 1039 cm^{-1} ($–SO_3^-$ stretching) and 1360 cm^{-1} (O═S═O stretching in $–SO_3H$) indicated that sulfonic acid groups were grafted onto the material surface.[22,24] The appearance of peaks at 2938 cm^{-1} and 2884 cm^{-1} are assigned to the stretching and vibration of NH_2 groups (Fig. 1);[25,26] absorption band at 1550 cm^{-1} is attributed to N–H stretching in amines, indicating that the solid had reacted with NH_2 *via* solvothermal reaction in DMA and carbonization in N_2 gas.[26] X-ray diffraction patterns (Fig. 2) showed presence of carbon, NiO and Ni, indicating that Ni(II) in the precursor was converted to metallic Ni after solvolysis. Diffraction peaks could be assigned to NiO (2θ = 36.7°, 42.7°, 62.3°, 74.9° and 79.0°) and metallic nickel (2θ = 45.0°, 52.8° and 76.2°) according to the literature.[27] Both Ni and NiO phase have face-centered cubic (fcc) crystal structure with $Fm\bar{3}m$ (225) space group,[27] so that based on peak shape parameters obtained by Rietveld refinement, the NiO and Ni crystallites were estimated to have sizes of 15.5 nm and 18.1 nm, respectively, which were calculated from the Debye–Scherrer formula using full width at half maximum in the peak.

The C 1s, N 1s, S 2p and O 1s core-level spectra binding energies are shown in Fig. 3 and S1.† Peaks with binding energies at 163.9 eV, 166.1 eV and 168.8 eV correspond to oxidized sulfur groups and those at 162 eV correspond to the thiol group (Fig. 3a).[28] Peaks with binding energies at 284.6 eV (C–N), 286.1 eV (C–O), 288.6 eV (O–C═O) and 400.9 eV (HNC═O) were observed[28] demonstrating that –COOH, $–NH_2$, and $–SO_3H$ groups were introduced into the as-prepared catalyst. The O 1s feature can be fitted by three peaks, at 529.3 eV, 531.6 eV and 533. 4 eV (Fig. S1†),[29] corresponding to the Ni–O, O–H and O–N/O–C bonds and XPS area ratios being 33.4%, 59.3% and 7.4%, respectively, which can be clearly assigned to the presence of both NiO and hydroxide species (OH/COOH/sulfate) in the catalyst. The binding energy of the obtained XPS spectra were charge corrected, and the existence of Ni 2p peaks that can be assigned to Ni^0 and NiO (Fig. 3d).[30,31] XRD and XPS results show that Ni^0 was reduced in the procedure. Namely, Ni(II) was reduced to zero-valent Ni in the synthesis conditions *via* carbon and organic ligands.[32,33] The results of the XPS spectroscopy and FT-IR spectra indicated the presence of Lewis and Brønsted acidic sites in the as-prepared catalyst.[34] SEM images (Fig. 4a) of the material showed aggregates of interconnected filaments (10 to 50) nm in size that showed that the as-prepared catalyst consisted of nanofibers. The SEM-EDX spectroscopy of the material (Fig. S2†) showed that the Ni and S were homogeneously dispersed on the surface of the as-prepared material with concentrations of 4% and 21%, respectively. TEM images (Fig. 4b) showed that Ni metal was dispersed in the as-prepared material and that it had small sizes (<20 nm) (Fig. 4). Total site acidity of the material was 5.5 mmol g^{-1} which was similar to Amberlyst-15 ion exchange resin (4.7 mmol g^{-1}). Moreover, the concentration of the primary Brønsted acid sites ($–SO_3H$) was 5.0 mmol g^{-1}, which was calculated from elemental analysis results, provided a Lewis acid/Brønsted acid site ratio of 1/10. TG-DTA results of the solids showed low mass loss below 500 °C, so that changes observed with temperature can be attributed to physically adsorbed water (Fig. S3†).

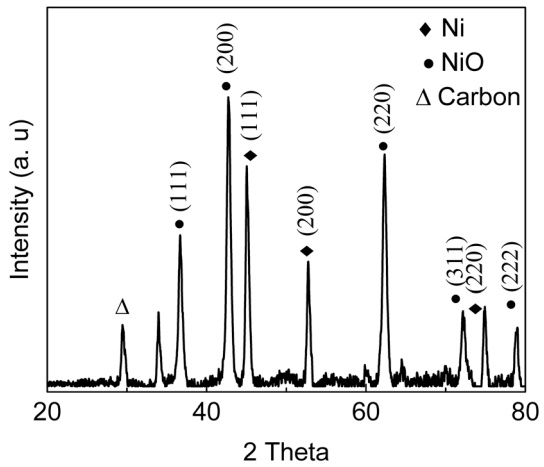

Fig. 2 XRD pattern of as-prepared bifunctional carbon Ni/NiO nanofiber catalysts.

3.2. Catalyst activity

To confirm the activity of the as-prepared solids, conversion of C5/C6 carbohydrates into ethyl levulinate was examined (Table 1). Furfuryl alcohol esterification–dehydration and LA etherification reactions with ethanol were first performed with the as-prepared solid to establish the acidity present in the catalyst (Scheme 1). When furfuryl alcohol (FAL) substrate in ethanol solvent was used without catalyst (entry 1, Table 1), conversion was low and EL could not be detected. When FAL substrate in ethanol solvent was used with the as-prepared solids, conversion was greater than 90% and a moderate EL yield was obtained (entry 2, Table 1). Conversion with Amberlyst-15 after 2 h reaction was higher than 90% with 72% yields of EL (entry 3–4, Table 1). Sulfonated carbon without amino groups materials (S-FC) provides similar conversions[14] as those for as-prepared amino-sulfonated nanofiber catalyst of this work, but have lower EL yields (69%) at the same reaction conditions (entry 5, Table 1). Moderate yields were obtained when LA was used as substrate (entries 6–7, Table 1) with few byproducts. It is show that the as-prepared catalyst exhibited activity and selectivity in conversion of furfural alcohol and levulinic acid to ethyl levulinate, owing to the existing amino-sites and

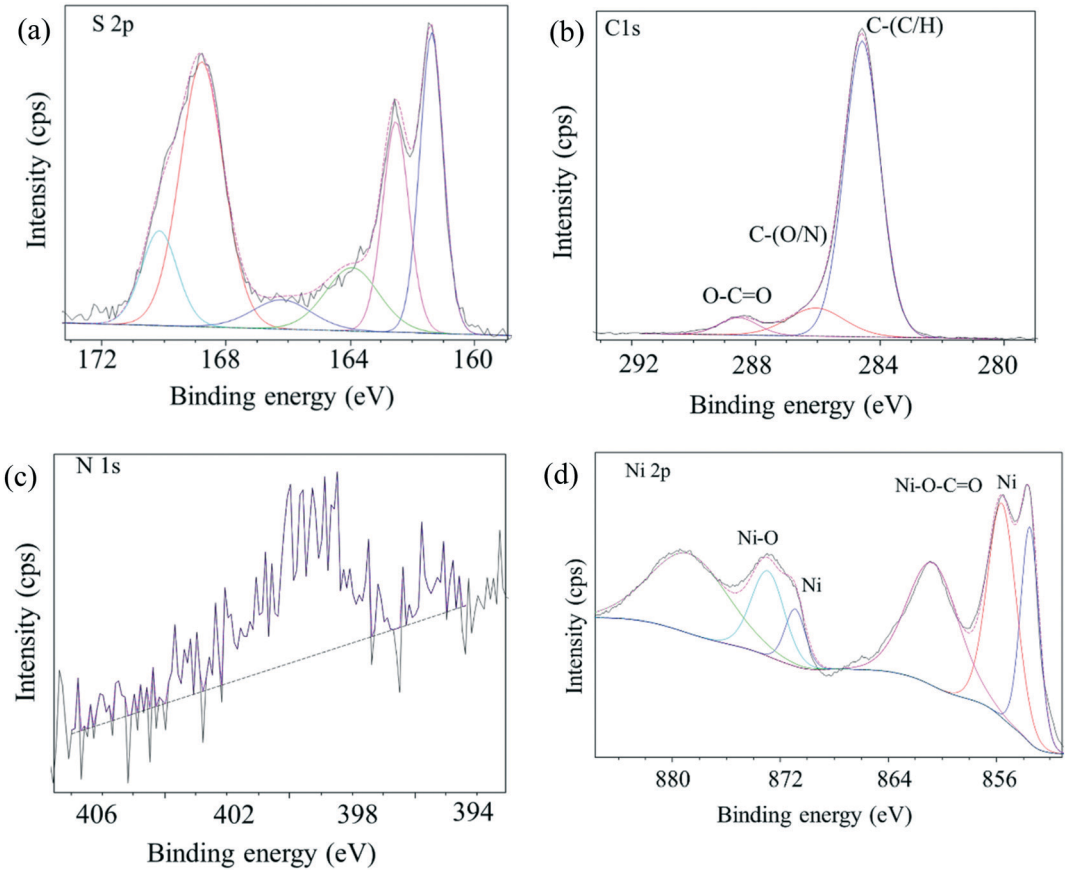

Fig. 3 XPS spectra of as-prepared bifunctional carbon Ni/NiO nanofiber catalysts. (a) XPS spectra of S 2p region, (b) XPS spectra of C 1s region, (c) XPS spectra of N 1s region, (d) XPS spectra of Ni 2p region.

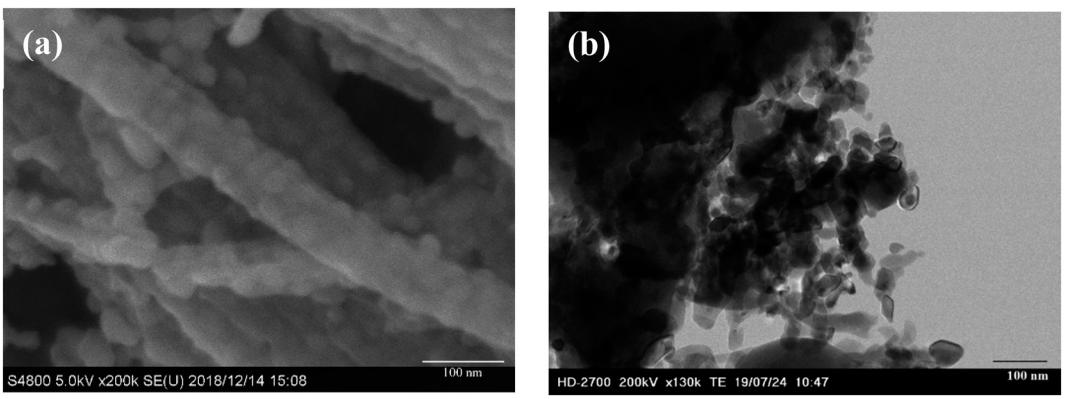

Fig. 4 As-prepared bifunctional carbon Ni/NiO nanofiber catalyst (a) SEM image and (b) TEM image.

Brønsted acid sites (–SO_3H), in which the Brønsted acid sites promoted etherification–dehydration reaction and the amino-sites exhibited a selective adsorption of substrates.[14] In the ATR-FTIR spectra (Fig. S4†), the band at about 3322 cm^{-1} is assigned to –OH groups in the monomeric FAL.[39] The –OH band shifted to higher wavenumbers when measurements were made with a mixture of FAL and catalyst, that is attributed strong interactions between hydrogen bonds between –OH groups in FAL and the catalyst. Adsorption experiments (Table S1†) showed that FAL preferentially adsorbed onto the amino-functionalized carbon catalyst over Amberlyst-15 or sulfonated carbon without amino groups (S-FC) suggesting that the amino groups enhanced interaction between Ni/NiO nanofiber catalyst and FAL through hydrogen bonding. Thus, it was concluded that the as-prepared solids had catalytic properties that are enhanced due to amino groups of the as-prepared solids promoting FAL oligomerization into 2,2′-difurfuryl ether[35] as characterized with ^1H NMR (Fig. S5†). Then, furfural the hydrogenation–esterification–dehydration reaction was performed with as-

Table 1 Synthesis of ethyl levulinate (EL) in ethanol with as-prepared Lewis Brønsted acid nanofiber catalyst. Products: ethyl levulinate (EL), furfural diethyl acetal (FDA), 5-hydroxymethylfurfural (5-HMF), 5-ethoxymethylfurfural (5-EMF) and 2-furan-acrolein (FUA)

Entry	Substrate	T (°C)	Time (h)	Conv. (%)	Product yield (%) EL	FDA	5-EMF	Ref.
1[a]	FAL	160	6	<15	0	—	—	This work
2	FAL	160	6	93	74	—	—	This work
3[b]	FAL	160	2	97	72	—	—	This work
4[b]	FAL	160	6	100	47			This work
5[c]	FAL	150	6	100	69			14
6	LA	120	5	87	71	—	—	This work
7[b]	LA	120	5	86	61	—	—	This work
8	Furfural	150	6	87	42	10	—	This work
9	Furfural	150	8	99	61	10	—	This work
10[b]	Furfural	150	8	100	5	<10	—	This work
11[d]	Furfural	140	4	16.9	15 FA		—	37
12[d]	Furfural	180	4	48.2	40 FA + FUA		—	37
13	Xylose	150	6	91	41	<4	—	This work
14	Fructose	140	24	99	49		12	This work
15	Glucose	140	24	94	<7	—	—	This work
16	Sucrose	140	24	98	26	—	—	This work
17	Inulin	140	24	—	9	—	41	This work
18	Cellulose	140	24	—	<5	—	—	This work

[a] Without catalyst. [b] Conditions: 0.05 g Amberlyst-15 instead of as-prepared catalyst. [c] Conditions: 0.06 g sulfonated carbon material, 6 mL of ethanol. [d] Conditions: 0.05 g RANEY® Ni, 0.2 g furfural, 15 mL ethanol, product: 2-furan-acrolein (FUA). Conditions: conversion of furfuryl alcohol (FAL) or furfural (0.1 g substrate, 0.05 g of as-prepared catalyst, 5 mL of ethanol); conversion of carbohydrates (xylose, fructose, glucose, sucrose, inulin or cellulose) 0.05 g substrates, 0.03 g catalyst, 4 mL ethanol.

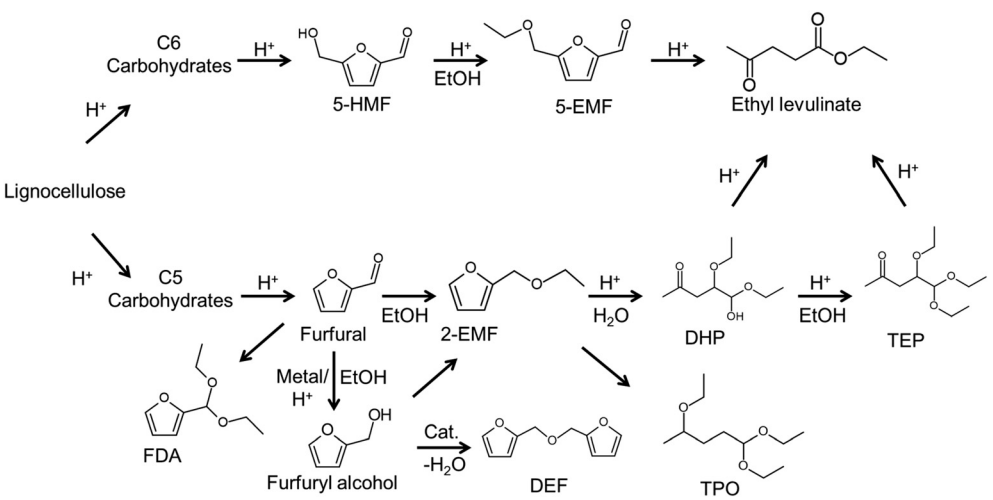

Scheme 1 Probable reaction pathway for the conversion of carbohydrates in ethanol over acid catalyst 5-hydroxymethylfurfural (5-HMF), 5-ethoxymethylfurfural (5-EMF), 2-(ethoxymethyl)furan (2-EMF), 2,2′-difurfuryl ether (DEF), furfural diethyl acetal (FDA), 4,5,5-triethoxypentan-2-one (TEP), 4,5-diethoxy-5-hydroxypentan-2-one (DHP) and 2,5,5-triethoxypentan-2-one (TPO).

prepared solid to further establish the transition metal present in the catalyst (entries 8–9, Table 1). A blank experiment was performed with Amberlyst-15 acid catalyst (entry 10, Table 1), at 150 °C, that gave high furfural conversions, but low product yields, which is a result of an acid-catalyzed reaction system in which furfural cannot undergo transfer hydrogenation to form furfuryl alcohol, but is favored to polymerize into humins and polymeric materials.[36] The results of the blank experiment with Amberlyst-15 provide evidence that the Lewis acidity sites of the as-prepared catalysts are active for the transfer hydrogenation reaction step. When furfural (entries 8–9, Table 1) and furfural-based substrate xylose (entry 13, Table 1) were used as substrate, EL yields were moderate with few byproducts, wherein ethanol acted as hydrogen donor in the hydrogenation step and as substrate in the etherification step. For furfural conversion in ethanol with Ni-based catalysts that do not contain $-SO_3H$ groups, the total selectivity of furfuryl alcohol and furan-2-acrolein is higher than 91% without ethyl levulinate formation,[37] which shows that Ni-based catalyst without $-SO_3H$ groups (*e.g.* RANEY® Ni) are active for the hydrogenation step, but are poor for

promotion of the etherification–dehydration step required to form ethyl levulinate. Due to excess ethanol being used with the as-prepared solids, furfural not only undergoes transfer hydrogenation into furfuryl alcohol but was also partially acetalized with ethanol into 2-furaldehyde diethyl acetal. Therefore, conversion of C5 carbohydrates to form EL *via* hydrogenation–etherification–dehydration can proceed in one-pot with the as-prepared solids that act as bifunctional catalysts. Comparing EL obtained with Amberlyst-15 strongly acidic cation exchange resin (entries 3, 4, 6, 10, Table 1), the bifunctional catalyst tended to give higher selectivity for EL at similar reaction conditions, which can probably be attributed to the presence of its functional groups (–NH_2, –COOH and –OH),[38] since the amino groups in the catalyst assist in activating the nucleophilic character of alcohols and in eliminating water molecules.[2] In the reaction pathway (Scheme 1), the as-prepared carbon Ni/NiO nanofiber catalyst stabilizes the reactant (*e.g.* furfural) *via* presence of its functional groups (–NH_2, –COOH and –OH), while the Lewis sites (Ni/NiO metal) promote furfural hydrogenation and the Brønsted acidity sites (–SO_3H groups) promote etherification into 2-ethoxymethylfuran that is followed by dehydration into ethyl levulinate.

Direct production of EL from other C6 carbohydrates was investigated using the as-prepared catalyst (entries 14–18, Table 1), where it can be seen that total yield of EL and 5-ethoxymethylfurfural (5-EMF) were relatively high (entries 14 and 16, Table 1) for fructose-related C6 carbohydrates compared with glucose-related C6 carbohydrates (entries 15–18, Table 1) although both could be directly converted into products (EL or 5-EMF) with the bifunctional catalyst. Limited EL yields for glucose-related C6 carbohydrates including cellulose can be attributed to glucose undergoing ethanolysis with ethanol to form ethyl-D-glycopyranoside (EDGP)[40] rather than isomerization into fructose in ethanol. It can be concluded that the conversion of C6 carbohydrates into EL *via* dehydration–ethanolysis steps can proceed in a one-pot reactor over the as-prepared catalyst and that the as-prepared solids have bifunctionality that can promote multiple reaction sequences of C5/C6 carbohydrates.

3.3. Reaction temperature and reaction time

Based on the above experimental results, conversion of furfural alcohol into ethyl levulinate was examined at several conditions (Fig. 5) in which carbon balances obtained at different temperatures are shown in Table S2.† Reaction temperature had a large effect on the conversion of furfural alcohol and the corresponding ethyl levulinates yields. When experiments were conducted at 130 °C, FAL conversion was low (8%) (Fig. 5a) and formation of EL (Fig. 5b) was not observed. At 140 °C, FAL conversion and EL product selectivity increased, while formation of etherified esters 2-EMF and TEP were observed (Scheme 1 and Fig. S6†). Reactions at (150 and 160) °C showed the same trends as

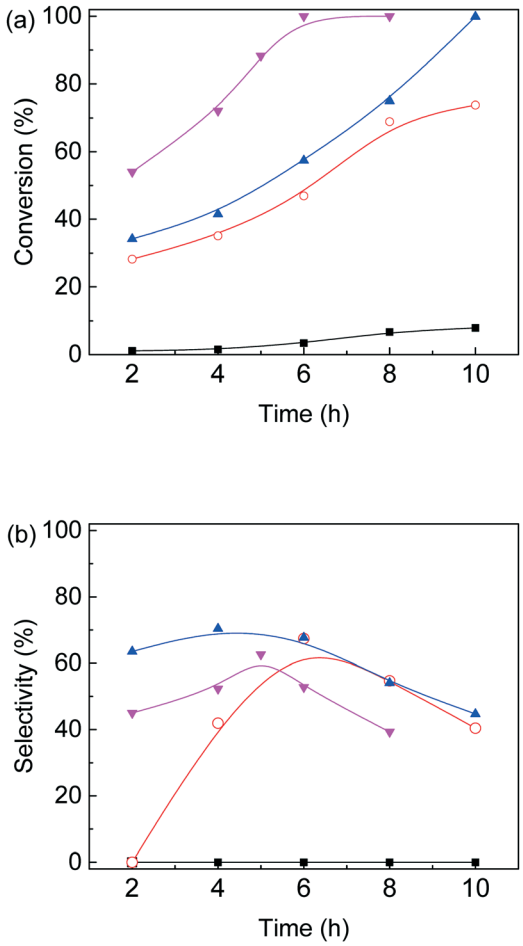

Fig. 5 Effect of reaction temperature and time on (a) furfural alcohol conversion and (b) ethyl levulinate selectivity for furfural alcohol etherification–hydrolysis catalyzed by as-prepared nanofiber catalyst in ethanol, black square: 130 °C; red circle: 140 °C; blue triangle: 150 °C and magenta downward triangle: 160 °C (0.1 g furfural alcohol, 0.05 g catalyst, 3 mL ethanol).

those at 140 °C, namely, EL selectivity exhibited a maximum with reaction time (Fig. 5), however, formation of desirable products (EL) was somewhat higher at 150 °C (71%) for 6 h reaction time (Table S2†). Further increase of reaction temperature to 160 °C, gave poor carbon balances (Table S2†) indicating that side reactions were promoted along with increasing amounts of unidentified byproducts. In summary, an increase in reaction temperature over 140 °C lead to an increase in FA conversion, but with a corresponding increase in byproducts. Variation of product selectivity with reaction conditions for conversion of FAL into EL in ethanol was examined (Fig. 5). Conversion of furfuryl alcohol into EL proceeds through the relatively stable intermediates 2-(ethoxymethyl)furan and 4,5,5-triethoxypentan-2-one.[16] Long reaction times tended to allow further conversion of EL into side-products such as levulinic acid and γ-valerolactone,[32,41] whereas high reaction temperature tended to promote formation of EL, but parallel conversion of FAL to 2,5,5-triethoxypentan-2-one.[16]

3.4. Catalyst loading

The effect of catalyst loading on FAL conversion into EL is shown in Fig. 6. When catalyst loading was increased from 0.03 g to 0.05 g, EL selectivity increased from 37% to 87% and FAL conversion increased, while byproduct selectivity remained lower than about 10%. As catalyst loading was increased further (>0.05 g), EL selectivity decreased, which is ascribed to an excess of acidity sites that promote dehydrogenation of furfuryl alcohol to form 2,2-difurfuryl ether and promote conversion of intermediates 2-EMF and 4,5,5-triethoxypentan-2-one into 2,5,5-triethoxypentan-2-one.

3.5. Catalyst scope

The scope of the bifunctional catalyst for different kinds of alcohol as both solvent and hydrogen donor source in FAL conversion to levulinate esters (LE) was examined (Table 2). As shown (entries 1–5, Table 2), the bifunctional catalyst was active for promoting all alcoholysis reactions. An increase in alkyl chain length of the alcohol (entries 1–5, Table 2) gave a decrease in LE selectivity and FAL conversion. Methanol and ethanol were the best performing solvents (Table 2), while the rest of the alcohols did not follow trends according to their chemical acidity (pK_a), such that selectivities may be related to hydrogen donor capabilities or possible inhibition of catalytic sites by alkoxy groups.[42,43]

Conversion of FAL to EL was studied for varying amounts of ethanol (entries 2, 6–8, Table 2), where conversions increased with increasing amount of ethanol solvent, and the EL selectivity exhibited a maximum (entry 2, Table 2). The presence of a maximum in EL selectivity with the amount of ethanol used in the reaction is possibly due to the esterification being an equilibrium reaction, so that increasing one of the reactant amounts (*e.g.* ethanol) favors product (*e.g.* EL) formation. However, increased ethanol concentration in the reaction system also lowers catalyst concentration, as shown by results in section 3.4 so that lower catalyst concentrations lead to lower EL selectivities, and this is possibly due to low catalyst concentration promoting the formation of intermediates 4,5,5-triethoxypentan-2-one and byproduct 2,5,5-triethoxypentan-2-one as observed in acid catalyzed reaction pathways (Scheme 1).[16,35]

Table 2 Conversion of furfuryl alcohol to levulinate esters (LE) with as-prepared Lewis Brønsted acid nanofiber catalyst in alcohol solvents. Products: methyl levulinate (ML), ethyl levulinate (EL), 1-propyl levulinate (POL), 1-butyl levulinate (BL), 1-pentyl levulinate (PEL) (reaction conditions: 0.1 g furfuryl alcohol, 0.05 g of catalyst, reaction temperature, 150 °C, reaction time, 6 h)

Entry	Alcohol	Molar ratio Alcohol/FAL	LE Product	Conv%	Select%
1	Methanol	50	ML	67.4	93
2	Ethanol	50	EL	67.0	93
3	1-Propanol	50	POL	71.2	39
4	1-Butanol	50	BL	73.0	34
5	1-Pentanol	50	PEL	68.1	28
6	Ethanol	16.7	EL	26.1	16
7	Ethanol	50	EL	57.4	88
8	Ethanol	84	EL	86.2	79
9	Ethanol	117	EL	91.7	79

3.6. Catalyst recycle and reuse

Catalyst recycle and reuse of the bifunctional catalyst were examined (Fig. 7). After reaction, the catalyst was separated by centrifugation and washed repeatedly with water–ethanol solutions. After drying at 80 °C under vacuum, the catalyst was used for the next run at identical conditions. FAL conversion remained constant for five recycles and EL selectivity slightly decreased (*ca.* 1%) in the first three

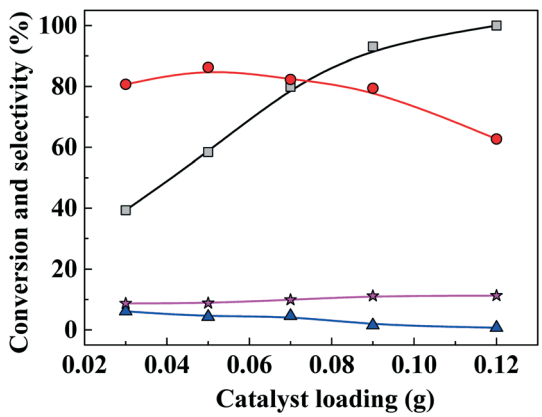

Fig. 6 Furfuryl alcohol conversion and ethyl levulinate (EL) selectivity *versus* catalyst loading for one-pot etherification–hydrolysis of furfuryl alcohol (FAL) with as-prepared nanofiber catalyst in ethanol. Reaction conditions: 0.1 g furfural alcohol, 3 mL ethanol, reaction temperature, 150 °C, reaction time, 6 h. Gray line and squares: FAL conversion; red line and circles: EL selectivity; blue line and triangles: 2-(ethoxymethyl) furan (2-EMF) selectivity; purple line and stars: 4,5,5-triethoxypentan-2-one (TEP) selectivity.

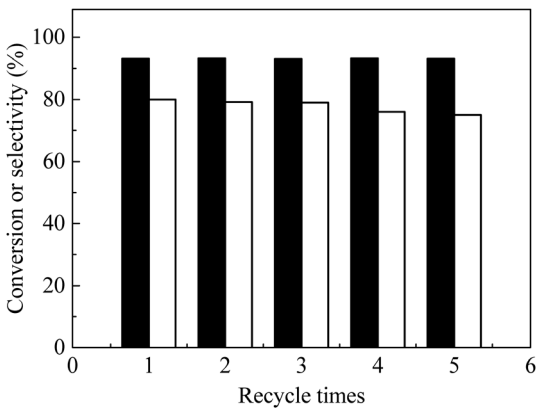

Fig. 7 Recycle of catalyst to obtain ethyl levulinate (EL) direct from furfural alcohol (FAL) with bifunctional nanofiber catalyst. Reaction conditions: 0.1 g FAL, 0.09 g catalyst, 3 mL ethanol, reaction temperature, 150 °C, reaction time, 6 h. Black bars: FAL conversion, white bars: EL selectivity.

recycles and about 5% overall after five recycles (Fig. 7), which indicated that the as-prepared catalyst was stable. TG-DTA of the spent catalyst (Fig. S7a and S3†) showed presence of humin precursors that probably reduced catalyst activity. FT-IR spectra of the spent catalyst (Fig. S7b†) showed that its functional groups (*e.g.* COOH, OH, amino groups) were similar to those of the as-prepared carbon solids. The loss of nickel metal in each step of the recycle was examined through several trials, in the products, in which less than 1% of nickel metal was concluded to be lost. Nevertheless, the as-prepared catalyst was determined to be active and stable after five times recycle.

4. Conclusions

A simple method was developed for synthesizing a bifunctional Ni/NiO carbon catalyst that has Lewis and Brønsted acidity. Morphology of the catalyst was nanofibers that were dispersed with functional groups. The prepared bifunctional catalyst is active for promoting C5/C6 carbohydrates in ethanol into ethyl levulinate *via* hydrogenation–etherification–dehydration reactions and it can be applied to form other levulinate esters. The bifunctional catalyst exhibited good stability and is reusable for at least five recycles.

Conflicts of interest

The authors declare that they have known competing financial interest or personal relationships that could have appeared to influence the work reported in this paper.

Acknowledgements

The authors are grateful for financial support from the JSPS Grant in Grant-in-Aid for Early-Career Scientists (No. 19K15347) and from the Materials Processing Science project ("Materealize") of the Ministry of Education, Culture, Sports, Science and Technology (MEXT), Grant Number JPMXP0219192801. H. G. gratefully acknowledges support from Tohoku University from the Program Center for Gender Equality Promotion.

References

1 L. T. Mika, E. Csefalvay and A. Nemeth, *Chem. Rev.*, 2018, **118**, 505–613.
2 Y. B. Huang, T. Yang, M. C. Zhou, H. Pan and Y. Fu, *Green Chem.*, 2016, **18**, 1516–1523.
3 R. Wang, X. Liang, F. Shen, M. Qiu, J. Yang and X. Qi, *ACS Sustainable Chem. Eng.*, 2020, **8**, 1163–1170.
4 H. Guo, A. Duereh, Y. Su, E. J. M. Hensen, X. Qi and R. L. Smith Jr, *Appl. Catal., B*, 2020, **264**, 118509.
5 Q. Girka, B. Estrine, N. Hoffmann, J. Le Bras, S. Marinkovic and J. Muzart, *React. Chem. Eng.*, 2016, **1**, 176–182.
6 F. Shen, S. Sun, X. Zhang, J. Yang, M. Qiu and X. Qi, *Cellulose*, 2020, **27**, 3013–3023.
7 H. Guo, A. Duereh, Y. Hiraga, T. M. Aida, X. Qi and R. L. Smith, Jr., *Chem. Eng. J.*, 2017, **323**, 287–294.
8 M. M. Zainol, N. A. S. Amin and M. Asmadi, *Fuel Process. Technol.*, 2017, **167**, 431–441.
9 E. I. Gurbuz, J. M. R. Gallo, D. M. Alonso, S. G. Wettstein, W. Y. Lim and J. A. Dumesic, *Angew. Chem., Int. Ed.*, 2013, **52**, 1270–1274.
10 G. Morales, J. A. Melero, J. Iglesias, M. Paniagua and C. Lopez-Aguado, *React. Chem. Eng.*, 2019, **4**, 1834–1843.
11 H. Guo, S. Tomoka and R. L. Smith, Jr., *J. Supercrit. Fluids*, 2020, **164**, 104891.
12 I. Lawan, W. M. Zhou, A. L. Idris, Y. F. Jiang, M. X. Zhang, L. W. Wang and Z. H. Yuan, *Fuel Process. Technol.*, 2020, **198**, 11.
13 S. S. Gori, M. V. R. Raju, D. A. Fonseca, J. Satyavolu, C. T. Burns and M. H. Nantz, *ACS Sustainable Chem. Eng.*, 2015, **3**, 2452–2457.
14 H. Guo, Y. Hirosaki, X. Qi and R. L. Smith Jr, *Renewable Energy*, 2020, **157**, 951–958.
15 Z. Babaei, A. N. Chermahini and M. Dinari, *Chem. Eng. J.*, 2018, **352**, 45–52.
16 G. M. G. Maldonado, R. S. Assary, J. A. Dumesic and L. A. Curtiss, *Energy Environ. Sci.*, 2012, **5**, 8990–8997.
17 J. F. Ma, J. Yang and J. F. Liu, *Acta Crystallogr., Sect. E: Struct. Rep. Online*, 2003, **59**, m481–m482.
18 T. Z. Forbes and S. C. Sevov, *Inorg. Chem.*, 2009, **48**, 6873–6878.
19 J.-F. Ma, J. Yang, L. Li, G.-L. Zheng and J.-F. Liu, *Inorg. Chem. Commun.*, 2003, **6**, 581–583.
20 Y. Yang, P. Du, J. F. Ma, W. Q. Kan, B. Liu and J. Yang, *Cryst. Growth Des.*, 2011, **11**, 5540–5553.
21 X. H. Qi, N. A. Liu and Y. F. Lian, *RSC Adv.*, 2015, **5**, 17526–17531.
22 H. X. Guo, X. H. Qi, L. Y. Li and R. L. Smith Jr, *Bioresour. Technol.*, 2012, **116**, 355–359.
23 S. S. R. Gupta and M. L. Kantam, *Catal. Commun.*, 2019, **124**, 62–66.
24 J. F. Yang, H. Y. Zhang, Z. F. Ao and S. F. Zhang, *Catal. Commun.*, 2019, **123**, 109–113.
25 J. Z. Chen, R. L. Liu, Y. Y. Guo, L. M. Chen and H. Gao, *ACS Catal.*, 2015, **5**, 722–733.
26 F. Zhang, H. Y. Jiang, X. Y. Li, X. T. Wu and H. X. Li, *ACS Catal.*, 2014, **4**, 394–401.
27 X. M. He, Y. R. Xu, X. J. Yao, C. W. Zhang, Y. Pu, X. F. Wang, W. W. Mao, Y. W. Du and W. Zhong, *RSC Adv.*, 2019, **9**, 30195–30206.
28 B. Quan, S. H. Yu, D. Y. Chung, A. Jin, J. H. Park, Y. E. Sung and Y. Piao, *Sci. Rep.*, 2014, **4**, 5639.
29 H. Yin, J. Zhu, J. Chen, J. Gong and Q. Nie, *Mater. Lett.*, 2018, **221**, 267–270.
30 H. J. Wang, X. D. Li, X. C. Lan and T. F. Wang, *ACS Catal.*, 2018, **8**, 2121–2128.
31 L. J. Yang, X. C. Zhao, R. Z. Yang, P. X. Zhao, Y. T. Li, P. Yang, J. C. Wang and D. Astruc, *Appl. Surf. Sci.*, 2019, **491**, 294–300.
32 H. X. Guo, Y. Hiraga, X. H. Qi and R. L. Smith Jr, *J. Supercrit. Fluids*, 2019, **147**, 263–270.

33 X. Y. Zhang, P. Gu, X. Y. Li and G. H. Zhang, *Chem. Eng. J.*, 2017, **322**, 129–139.
34 S. Q. Xu, C. Y. Yin, D. H. Pan, F. Hu, Y. F. Wu, Y. A. Miao, L. J. Gao and G. M. Xiao, *Sustainable Energy Fuels*, 2019, **3**, 390–395.
35 R. S. Malkar, H. Daly, C. Hardacre and G. D. Yadav, *React. Chem. Eng.*, 2019, **4**, 1790–1802.
36 X. Hu, C. Lievens and C. Z. Li, *ChemSusChem*, 2012, **5**, 1427–1434.
37 H. G. Zhang, X. L. Tong, Y. Q. Gao, H. Chen, P. F. Guo and S. Xue, *J. Ind. Eng. Chem.*, 2019, **70**, 152–159.
38 F. G. Cirujano, A. Corma and F. Xamena, *Catal. Today*, 2015, **257**, 213–220.
39 E. E. M. Ahmad, A. S. Luyt and V. Djokovic, *Polym. Bull.*, 2013, **70**, 1265–1276.
40 H. Li, S. Saravanamurugan, S. Yang and A. Riisager, *Green Chem.*, 2016, **18**, 726–734.
41 S. Song, S. K. Yao, J. H. Cao, L. Di, G. J. Wu, N. J. Guan and L. D. Li, *Appl. Catal., B*, 2017, **217**, 115–124.
42 H. Shafaghat, I. G. Lee, J. Jae, S. C. Jung and Y. K. Park, *Chem. Eng. J.*, 2019, **377**, 8.
43 X. Y. Wang and R. Rinaldi, *Energy Environ. Sci.*, 2012, **5**, 8244–8260.